International Conference on Renewable Energies and Power Quality (ICREPQ'18)
Salamanca (Spain), 21th to 23th March, 2018
Renewable Energy and Power Quality Journal (RE&PQJ)
ISSN 2172-038 X, No.16 April 2018

# Influence of fault impedance on voltage quality in radial distribution systems with distributed synchronous generator: a sensitivity analysis

A. J. T. S. Filho[1], A. O. Camargo[2] and E. G. Domingues[1,2,3]

[1] Faculty of Control and Automation Engineering
[2] Faculty of Electrical Engineering
[3] Nucleus of Experimental and Technological Studies and Research (NExT)
Federal Institute of Goiás, IFG
Campus Goiânia – Goiás, Brazil
Phone/Fax number: +556232272769, e-mail: ajtsfilho@gmail.com, nosrednaoc@gmail.com, prof.eldergd@gmail.com

**Abstract. The power quality delivered to final consumers has deserved special attention on the part of the scientific community due to the increasing deterioration of voltage and current waveforms as a result of use of non-linear loads. Deployment of Distributed Generation Power is expected to have a range of effects (positive or negative) on the distribution grid. This paper presents a sensitivity analysis of voltage quality of a radial distribution system located in Guarulhos, Brazil, in a presence of a distributed synchronous generator in one of its bars. The sensitive analysis is done by varying the resistive fault impedance by considering the occurrence of different types of faults due to atmospheric discharging. The system is modelled and simulated in time domain through ATP software. It was verified that the impacts caused by the symmetrical and asymmetric faults on voltage levels are attenuated as the resistive fault impedance increases.**

**Key words:** ATP software, fault impedance, sensitivity analysis, voltage quality.

## 1. Introduction

In the last two decades, the world's electrical sectors have been marked by the growth of non-linear loads and by the insertion of sensitive devices and processes, which are affected by problems related with power quality.

Moreover, the growing need for electrical power and the greater awareness of the environmental issues have led to an increase of the Distributed Generation (DG) from renewable sources (sun, wind and biomass) in the distribution systems.

A high level of DG penetration in the distribution systems may lead problems due to the lack of the power quality. Currently, the sector lives in a period of great learning concerning these kinds of generation and their technical and economic impacts.

Among the phenomena treated in the scope of the power quality, voltage quality deserves special attention due to financial loss in the commercial and industrial sectors, which come from: a) burn of devices, and b) malfunctioning of sensitive devices, which may lead to industrial stoppages, loss of raw material and due to long periods of process shutdown.

The short-duration voltage variations (SDVVs) are characterized by variations in the voltage mainly caused by: i) faults in the grid, which may lead to reductions (voltage sags) or elevations (voltage swells); and ii) starting of large loads, connected to the distribution systems (e.g. the start of large motors), due to high transitory current levels.

According to IEEE Std 846 [1], voltage sag is defined as a decrease of RMS voltage from 0.1 to 0.9 p.u., duration a time interval of 0.5 cycle to 1 minute. Voltage swell is defined as the increase in the RMS voltage value from 1.1 to 1.8 p.u. for duration of 0.5 cycle to 1 minute. If the RMS voltage drops below 0.1 p.u., the event is considered as a short duration interruption.

In the Brazilian case, the eight module of the Distribution Procedures (PRODIST) classifies the SDVVs in momentary variations, for durations up to 3 s; and temporary voltage variations (TVV), for durations from 3 s to 3 min. According to PRODIST, voltage interruptions are classified from 0 to 0.1 p.u., voltage sags occurs from 0.1 p.u. to 0.9 p.u. and for voltage swells any variation above 1.1 p.u..

Some factors influence the characteristics of sags such as: pre-fault voltage, fault location, fault type, protection systems, reclosing systems and fault impedance [2].

The faults that occur in electrical grids are mainly caused by burns, trees close to conductors, loss of line insulation, mechanical failures and atmospheric discharges. Faults from atmospheric discharges are the main cause of the non-programmed disruptions in transmission lines and occur due to the directly or indirectly incidence of atmospheric discharges. This type of fault occurs due to the establishment of overvoltages in the insulator chains, or between its conductors, that end up disrupting its insulation. In the case of atmospheric discharges, which are the main cause for short circuits, the fault resistance may be represented as a resistance of the electric arc, with typical values from 0 to 10 ohms. The fault impedance due to burns, falling of structures and trees has higher typical values, reaching up to 150 ohms when a tree drops on the line [3].

In a study developed by [4] voltage drops caused by faults on transmission lines, such as three-phase-ground (PPPE), phase-to-earth (PE) and phase-to-phase (PP) are presented. The presented methodology is a tool that is able to give a fast qualitative evaluation of the effect of the fault impedance in the phase angle jump of the voltage sag, and so determine the immunity of the sensitive device during such event.

The work developed in [5] presents the study of the models already developed and tested for high impedance faults in distribution systems, due to the disruption and drop of primary conductor in distribution grids, as well as develops computational interface to make feasible this kind of study, making it possible to validate protection schemes against high impedance faults.

The impact of the fault impedance on voltage sags is presented in [2]. The study uses the ANAFAS software to simulate and analyze the influence of the DG in the magnitude of the voltage sags obtained on bars.

In [6], a study on MATLAB/Simulink about the influence of the fault resistance in a three-phase fault is presented. Such work was able to show that the higher the fault resistance, the lower the magnitude of voltage sags.

In this context, the main objective of this paper is to do a sensitivity analysis of the voltage quality of a radial distribution system in the presence of a distributed synchronous generator by doing the variation of the resistive fault impedance considering the occurrence of different types of faults due to atmospheric discharging. The analysis is done, by using the ATP software, in an eight-bar radial system, located in Guarulhos, São Paulo, Brazil.

## 2. Methodology

Simulations were made through the software Alternative Transient Program – ATP, which is a flexible and important tool in the studies of transient phenomena in power systems.

ATP allows the simulation of poly-phase grids, using the bars admittance matrix. The mathematical formula used by the program is based, for elements with distributed parameters, on the method of characteristics (Bergeron's Method) and for concentrated parameters, on the trapezoidal rule integration [7].

The distribution system used in the simulations is presented in the unifilar diagram of the Figure 1 [8]. It is a radial distribution feeder of eigth bars, 13.8 kV, from the Bandeirante Power Distribution Company, located near to the airport of city of Guarulhos/SP, Brazil. The system is composed by one substation (SS), six balanced loads connected to the bars B1, B2, B3, B4, B5, B6 and B7, a line end bus (B8) and a distributed synchronous generator (DG) connected on bar B7.

The modeling of the distributed generator in the ATP software consisted in treating it as a series voltage source, with its synchronous reactance, represented by figure 1. The study also considered the distributed generator as supplying a power lower than the sum of the power of all the loads.

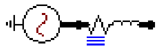

Figure 1 - DG representation (voltage source, resistance and synchronous inductance)

Knowing the values of the nominal voltage (U), the apparent power (S), the active power generated ($P_G$), the reactive power generated ($Q_G$), the armature resistance ($r_s$), the direct axis transient reactance ($x_s$) and the terminal voltage, it is possible to obtain the necessary parameters in order to model the distributed generator in the software ATP, according to the following equations from 1 to 6 [9]:

Base impedance:
$$Z_b = \frac{U^2}{S} \tag{1}$$

Synchronous resistance:
$$r_s(\Omega) = r_s(pu) \times Z_b \tag{2}$$

Synchronous reactance:
$$x_s(\Omega) = x_s(pu) \times Z_b \tag{3}$$

Inductance:
$$L = \frac{x_s(\Omega)}{2 \times \pi \times 60} \tag{4}$$

Generator internal voltage phase-angle:
$$\delta = \mathrm{arctg}\frac{P_G}{(Q_G + \frac{V_t^2}{x_s})} \tag{5}$$

Distributed generator internal voltage:
$$E_F = \frac{P_G \times x_S}{V_t \times \mathrm{sen}\ \delta} \tag{6}$$

Figure 1 ilustrates the unifilar diagram of an eight bar radial distribution system located next to the Airport of Guarulhos, São Paulo, Brazil.

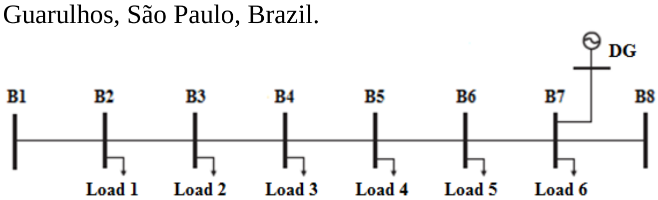


Figure 2 - Unifilar diagram of a eight bar radial distribution system (Adapted from [8])

Tables 1 to 4 present the electrical parameters of the components that compound the electric system [8]:

Table 1 – Parameters of the substation bus (SE)

| | |
|---|---|
| **Voltage** | 13.8 kV |
| **Short-circuit power** | 7.0 MW |
| **Phase-angle of the Substation** | 3.23º |

Table 2 - Parameters of the three-phase transmission lines

| Line | Length [m] | Conductor |
|---|---|---|
| **B1-B2** | 1000 | ACSR 336.4 |
| **B2-B3** | 3000 | ACSR 336.4 |
| **B3-B4** | 1000 | ACSR 336.4 |
| **B4-B5** | 500 | ACSR 336.4 |
| **B5-B6** | 500 | ACSR 336.4 |
| **B6-B7** | 1000 | ACSR 336.4 |

Table 3 - Characteristics of the loads – series-star connection

| Load | Active Power [kW] | Reactive Power [kVar] | R [Ω] | L [mH] |
|---|---|---|---|---|
| **Load 1** | 870 | 275 | 193.85 | 162.54 |
| **Load 2** | 800 | 255 | 196.81 | 166.40 |
| **Load 3** | 1160 | 370 | 133.05 | 112.57 |
| **Load 4** | 1260 | 400 | 121.66 | 102.45 |
| **Load 5** | 470 | 150 | 324.33 | 274.56 |
| **Load 6** | 2170 | 690 | 69.75 | 58.83 |

SOURCE: ADAPTED FROM [9].

Table 4 - Characteristics of the distributed generator [8]

| Parameter | Value |
|---|---|
| **Nominal voltage (U):** | 13,8 kV |
| **Apparent power (S):** | 3 MVA |
| **Actie power generated ($P_G$):** | 2700 kW |
| **Reactive power generated ($Q_G$):** | 1400 kVAr |
| **Armature resistance ($r_s$):** | 0.3% |
| **Direct axis transiente reactance ($x_s$):** | 40.8% |
| **Voltage on bus 7 (Vt):** | 12.89 kV |

Concerning the transmission lines, the conductor used in the simulation is the ACSR 336.4 form the manufacturer NEXANS. With the catalogue of the manufacturer it was obtained the values of: a) the resistance equal to 0.2051 Ω/km; b) the inductive reactance equal to 0.3770 Ω/km; and c) capacitive reactance equal to 0.2266 MΩ/km [10]. Using the technical data of the conductor, the electrical parameters of the distribution lines requested by the software ATP were obtained. The value of the electrical parameters of the distribution lines (π model) are presented in Table 5.

Table 5 - Parameters of the distribution lines

| Bar | Distance [m] | R [Ω] | L [mH] | C [μF] |
|---|---|---|---|---|
| **B1-B2** | 1000 | 0,2051 | 1,000 | 0,0117 |
| **B2-B3** | 3000 | 0,6153 | 3,000 | 0,0351 |
| **B3-B4** | 1000 | 0,2051 | 1,000 | 0,0117 |
| **B4-B5** | 500 | 0,1025 | 0,500 | 0,0058 |
| **B5-B6** | 500 | 0,1025 | 0,500 | 0,0058 |
| **B6-B7** | 1000 | 0,2051 | 1,000 | 0,0117 |
| **B7-B8** | 1000 | 0,2051 | 1,000 | 0,0117 |

Table 6 presents the electrical parameters of the distributed synchronous generator, according to the ATP model.

Table 6 - Parameters of the distributed synchronous generator

| Parameter | Value |
|---|---|
| **Base impedance ($Z_b$)** | 63.48 Ω |
| **Synchronous resistance ($r_s$)** | 0.19044 Ω |
| **Synchronous reactance ($x_s$)** | 25.899 Ω |
| **Synchronous inductance (L)** | 68.699 mH |
| **DG phase-angle (δ)** | 19.06° |
| **DG internal voltage ($E_F$)** | 16.61 kV |

After modeling the system showed in Figure 1, by using ATP software, it is possible vary the fault impedance and check how sensible is the bar voltages in relation to this parameter.

## 3. Results

Figure 3 illustrates an eight bar radial distribution system from the Bandeirante electric-power distribution company, located in São Paulo, Brazil. The system has rated voltage equal to 13.8 kV and a distributed synchronous generator equal to 3 MVA inserted on B7.

It was considered the occurrence of all types of faults on B7, namely: phase-to-phase (PP), phase-to-phase earth (PPE), three-phase earth (PPPE) and phase to earth (PE).

Sensitivity analysis of the magnitudes of short circuits in bus B7 and voltages in all bars were done by varying the values of the fault impedance located in bus B7.

The simulations were based on the following considerations: a) the fault impedance was considered as resistance, representing the electric arc resistance due to faults caused by atmospheric discharges. The values of such impedance can vary in a range of typical values from zero to 15 Ω with an increase rate of 1 Ω [2]; b) for the simulations of the PP and PPE faults, it was considered that the faults occur on phases B and C; c) for the PE faults, it was considered that the fault occur on phase C; d) the simulations were done with and without the presence of the DG in bus B7; and d) the magnitudes of faults and voltages presented in the simulations are RMS values, obtained after the system reach the steady state condition.

Figure 4 and Figure 5 show the behavior of the short-circuit levels of the PP, PPE, PPPE and PE types of faults on bar B7, without and with the presence of the DG, respectively. It can be notice that, in both cases, short-circuits levels decreases as the resistive fault impedance increases. The PPPE and PE short-circuits presented the

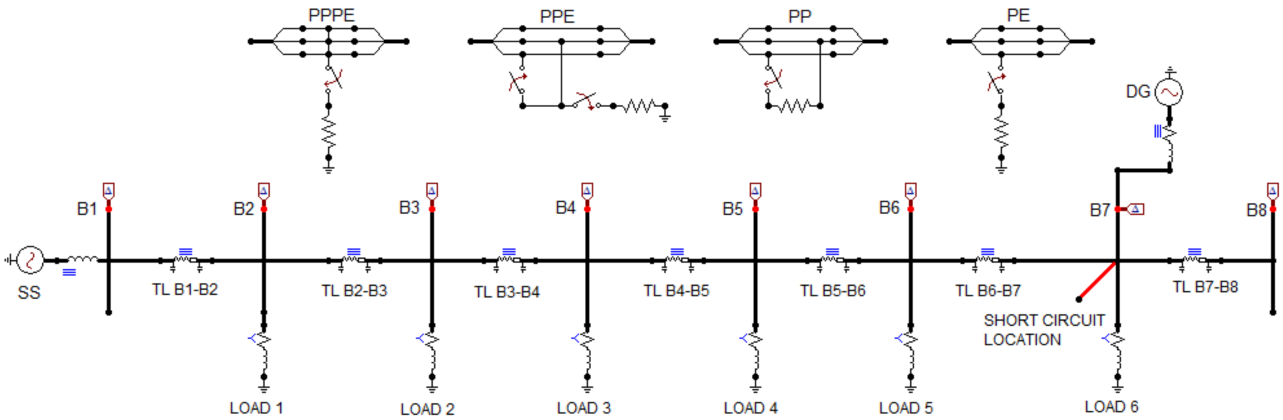

Figure 3 - Electrical system modeled in the ATP (Source: Author)

same values. As expected, the insertion of the DG led to higher short-circuit current levels. It occurs due to the fact that the both the substation and DG contribute to the short-circuit.

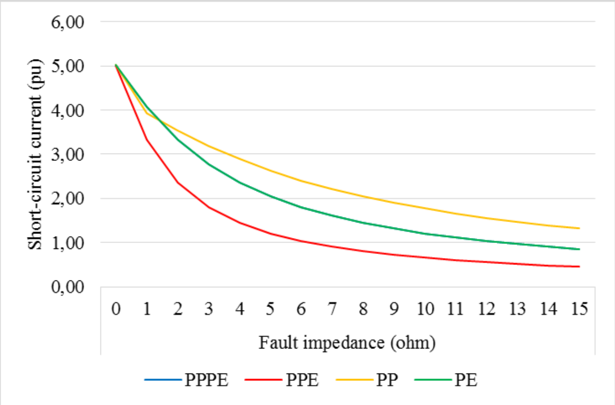

Figure 4 - Impact on the short-circuit levels on B7 without DG

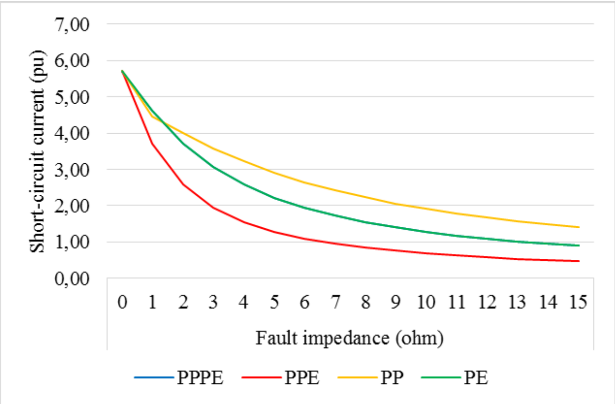

Figure 5 - Impact on the short-circuit levels on B7 with DG

Figure 6 shows the behavior of the RMS values of the line voltages in all bars of the system, as a function of the fault impedance and for the occurrence of a three-phase fault on B7.

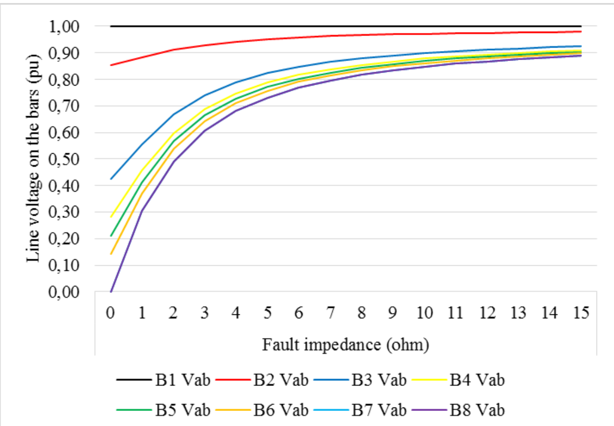

Figure 6 - Influence of the fault impedance on the line voltages of the bars (phase AB), for PPPE fault on B7

Note that the increase in the fault impedance contributes positively to the diminishment of the fault levels and, therefore, for the increase of the voltage levels in the bars. For impedance values equal to 0 Ω, bars 7 and 8 will suffer an interruption, while the other bars will probably have voltage sags if the system protection doesn't act correctly. It can be noticed that there will be a migration from the condition of interruption to the voltage sag condition for all bars, except on B1, as the fault impedance increases. Therefore, the increase in the fault impedance significantly decreases the impact on the voltage levels of the bars in the case of the PPPE fault.

For all cases, there was no voltage variation on B1 because this is an infinite bar (near the substation, inductance of $10^{-7}$ mH). The variation of the fault impedance did not influence the voltages on B1.

Figure 7, Figure 8 and Figure 9 illustrate the behavior of the RMS line voltages in all the bars, for the occurrence of the phase-phase fault (phases AB) on B7, as a function of the fault impedance.

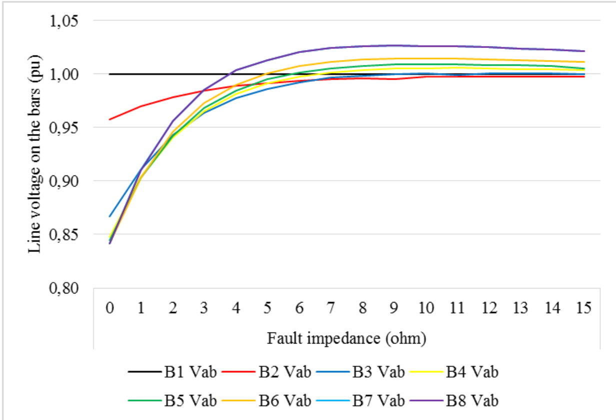

Figure 7 - Influence of the fault impedance on line voltages (phase AB) of the bars for the PP fault on B7

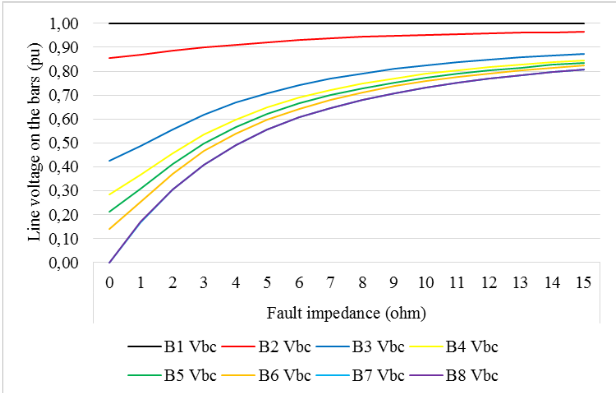

Figure 8 - Influence of the fault impedance on the line voltages (phase BC) of the bars for the PP fault on B7

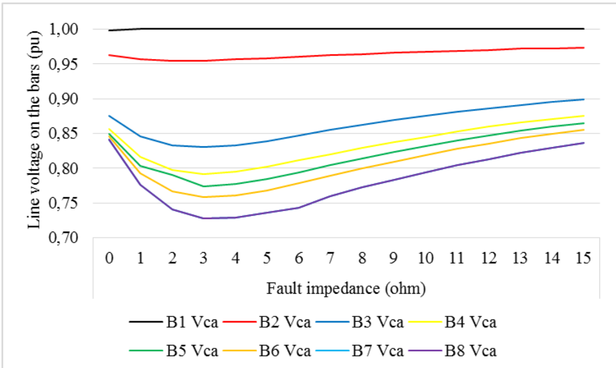

Figure 9 - Influence of the fault impedance on the line voltages (phase CA) of the bars for the PP fault on B7

It can be notice that, the increase in the fault impedance contributes to reduction of the short-circuit levels on B7 and for the improvement in the voltage levels on the bars.

The results presented in Figure 7 shows that the fault impedance contributed to the migration from the condition of voltage sag to the condition of voltage variations between 0.9 and 1.1 p.u., considered acceptable levels.

In Figure 8, the increase in the fault impedance on bar B2 collaborates to the change on the condition of voltage sags of 0.86 p.u. to the condition of voltage variation of 0.97 p.u.. All other bars remained under voltage sag, since their voltage levels are below 0.90 p.u..

It can be noticed on Figure 9 that the variation on the fault impedance lead to a voltage drop in the interval ranging from 0 to 3 Ω and a voltage raise in the interval between 3 Ω and 15 Ω. In this case, voltage sags remained except on bar B3, where there was a change to voltage variation condition, going from 0.88 p.u. to 0.90 p.u..

Figure 10, Figure 11 and Figure 12 present the behavior of the RMS values of the line voltages of the bars for a phase-to-phase fault (phases AB) on bar B7, as a function of the variation of the fault impedance. It can be noticed that, in general, the increase in the fault impedance contributes for the improvement on the voltage levels in all bars.

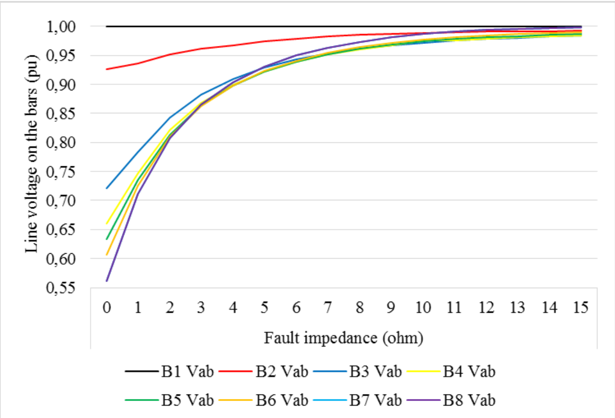

Figure 10 - Influence of the fault impedance on line voltages (phase AB) of the bars for the PPE fault on B7

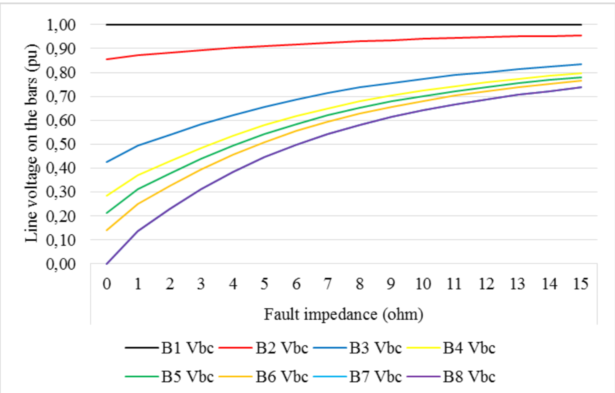

Figure 11 - Influence of the fault impedance on line voltages (phase BC) of the bars for the PPE fault on B7

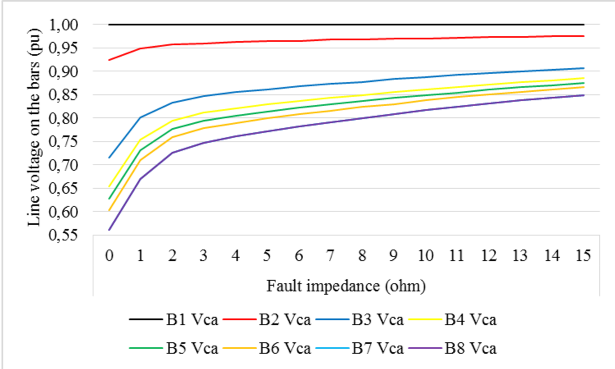

Figure 12 - Influence of the fault impedance on line voltages (phase CA) of the bars for the PPE fault on B7

Figure 10 shows that values of the fault impedance above 4Ω, led to a change of voltage sag condition to voltage variation condition.

Figure 11 shows that an increase in the fault impedance from 0 Ω to 15 Ω contributes to the change on the condition from voltage sag of 0.86 p.u. to a voltage variation of 0.95 p.u. on bar B2. The other bars remained in a voltage sag condition, although lower in intensity, reaching values from 0.74 p.u. to 0.83 p.u..

Figure 12 shows that an increase in the fault impedance from 0 Ω to 15 Ω contributes to the change on the condition from voltage sag of 0.71 p.u. to voltage variation of 0.92 p.u. on bar B3. Bars B4, B5, B6, B7 and B8 remained in a voltage sag condition, though lower in intensity reaching values from 0.85 p.u. to 0.88 p.u..

Figure 13, Figure 14 and Figure 15 illustrate the behavior of the RMS values of the line voltages in the bars for a phase-to-earth fault (phase C) on bar B7, as a function of the variation of the fault impedance. It can be noticed that there were virtually no significant changes in the RMS value of the line voltages on phases AB in the bars.

For the case of BC phases (affected phases), there was a voltage variation from 0.56 p.u. to 0.97 p.u.. Concerning the CA phase, the voltage changed from 0.56 p.u. to 0.89 p.u., so remaining as voltage sag.

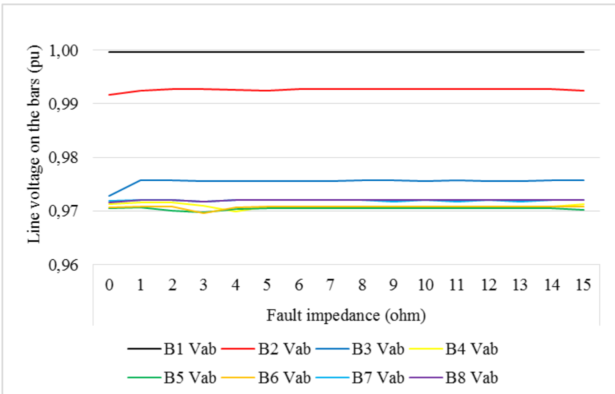

Figure 13 - Influence of the fault impedance on line voltages (phase AB) of the bars for the PE fault on B7

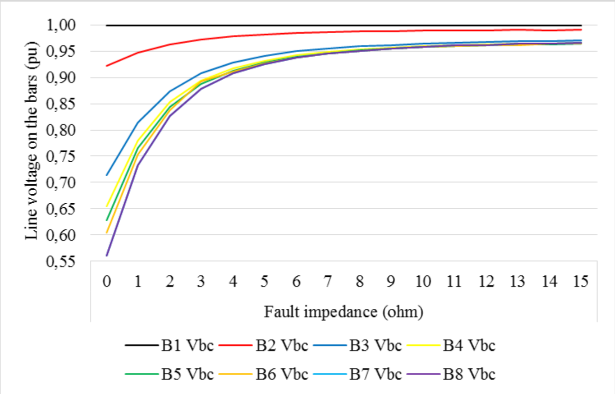


Figure 14 - Influence of the fault impedance on line voltages (phase BC) of the bars for the PE fault on B7

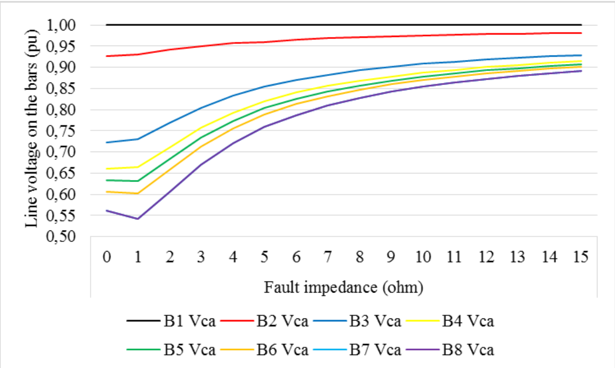


Figure 15 - Influence of the fault impedance on line voltages (phase CA) of the bars for the PE fault on B7

It can be noticed in Figure 13 that the increase in the fault impedance does not significantly affect the voltage levels on the bars for the phase AB, remaining practically unaltered.

According to Figure 14, fault impedance values greater than 4Ω, lead to the condition of voltage sag to a voltage variation condition.

Figure 15 shows that a value of 15 Ω on the fault impedance contributed to the migration from the condition of voltage sags on bars B3, B4, B5, B6 to a voltage variation, while bars B7and B8 remained under a voltage sag with a lower intensity of 0.89 p.u..

## 4. Conclusion

The results presented in this paper showed that as the resistive fault impedance increases for all types faults, in general, the short-circuits levels on bar 7 reduce and the RMS values of the voltages in the all bars increase.

As the true value of the fault impedance is difficult to obtain, it is usually to consider its value equal to zero. That condition corresponds to the highest levels of short circuits, as it has been confirmed in this paper. The protections devices are dimensioned for the worst possibility of fault level, seeking the highest level of security for the system.

From the obtained results, it can be observed that, for all types of simulated faults, the DG lead to a decrease in the severity of the voltage sags on the bar to which it is connected. It occurs due to the low level of short-circuit in the DG bar when compared to the substation bar (B1).

## References

[1] IEEE Std 846 “Recommended for Emergency and Standby Power Systems for Industrial and Commercial Applications”, IEEE Orange Book, 1995.

[2] A.C.L Ramos, A.J Batista, R.C Leborgne, P. Emiliano, “Distributed generation impact on voltage sags” Power Electronics Conference, 2009. COBEP '09. Brazilian, vol., no., pp.446-450, Sept. 27 2009-Oct. 1 2009.

[3] Cunha, L. V., “Performance of transmission lines against atmospheric discharges: influence of the corona effect on the rupture mid-span ", Master's Dissertation, Federal University of Minas Gerais, Belo Horizonte-MG, 2010.

[4] Kim, S. D., Morcos, M. M., Gomez, J. C., “Voltage-Sag Magnitude and Phase Jump due to Short Circuits in Distribution Systems with Variable Fault Resistance”, Electric Power Components and Systems, 33:5, 493-512, Oct 2005.

[5] Oliveira, D. A., “High Impedance Faults: Detection and location of conductor rupture in primary circuit of overhead distribution networks based on voltage unbalance ". Master’s Dissertation. Federal University of Minas Gerais, Belo Horizonte-MG, 2007.

[6] Farade, R., Kotiyal, B., Balsing, A. H., “Three-phase-to-ground fault and its impact on voltage magnitude” International Journal of Innovations in Engineering Research and Technology [IJIERT] (ISSN: 2394-3696), Volume 2, Issue 3, Mar 2015.

[7] Cabral, R. J., “ Numerical Analysis of Short Circuit using Symmetrical Components and Phase Components to Obtain Indices of Voltage Sags” Master’s Dissertation. Federal University of Rio Grande do Sul, Porto Alegre-RS, 2010.

[8] Lora, E. E. S.; Haddad, J., “Distributed Generation Technological, Environmental and Institutional Aspect”, Rio de Janeiro: Interscience, 2006.

[9] Peres, L. M., “Studies of the Dynamic Performance of Synchronous Generators of Independent Producers in Distributed Generation Systems via ATPDraw ", Master's Dissertation - Faculty of Electrical Engineering, Federal University of Uberlândia, Uberlândia-MG, 2013.

[10] NEXANS FICAP (2013). Aluminum. Available at: <http://www.nexans.com.br> Accessed on: 01/23/2017.